Research Article

Effects of Doping on the Performance of CuMnO$_x$ Catalyst for CO Oxidation

Subhashish Dey[1], Ganesh Chandra Dhal[1,*], Ram Prasad[2], Devendra Mohan[1]

[1]Department of Civil Engineering, Indian Institute of Technology (BHU) Varanasi, India
[2]Department of Chemical Engineering and Technology, Indian Institute of Technology (BHU) Varanasi, India

Abstract

The rare earth-doped CuMnO$_x$ catalysts were prepared by co-precipitation method. The CuMnO$_x$ catalyst was doped with (1.5 wt.%) CeO$_x$, (1.0 wt.%) AgO$_x$, and (0.5 wt.%) of AuO$_x$ by the dry deposition method. After the precipitation, filtration, and washing process, drying the sample at 110 ^{o}C for 16 hr in an oven and calcined at 300 ^{o}C temperature for 2 h in the furnace at stagnant air calcination condition. The influence of doping on the structural properties of the catalyst has enhanced the activity of the catalyst for CO oxidation. The doping of noble metals was not affected the crystal structure of the CuMnO$_x$ catalyst but changed the planar spacing, adsorption performance, and reaction performance. The catalysts were characterized by Brunauer-Emmett-Teller (BET) surface are, Scanning Electron Microscope Energy Dispersive X-ray (SEM-EDX), X-Ray Diffraction (XRD), and Fourier Transform Infra Red (FTIR) techniques. The results showed that doping metal oxides (AgO$_x$, AuO$_x$, and CeO$_x$) into CuMnO$_x$ catalyst can enhance the CO adsorption ability of the catalyst which was confirmed by different types of characterization technique. Copyright © 2017 BCREC Group. All rights reserved

1. Introduction

The catalytic oxidation of carbon monoxide (CO) is one of the important techniques which receiving a significant attention because of its applications in many different fields, i.e. respiratory protective devices, fuel cells, CO$_2$ laser gas generation, and automobile emission controls, etc. [1-2]. For controlling the pollution by vehicular emissions, the different type of catalysts has been used in the catalytic converter for CO oxidation process. In comparison between the noble and non-noble metal catalysts, the non-noble metal catalysts are available at low cost [3]. The hopcalite based CuMnO$_x$ catalyst was a well-known catalyst for CO oxidation at low temperature. The CuMnO$_x$ catalyst was attracted much attention because of its low cost, high catalytic activity, and moisture resistance [4].

There were many attempts made to improve the performance of CuMnO$_x$ catalyst by optimizing the preparation conditions and exploring new preparation method [5]. The precipitant effects on the crystalline phases of the catalyst while the precursor effect on the number of catalytic active sites and both are directly

---

* Corresponding Author.
  E-mail: ganesh.dhal@gmail.com (Dhal, G.C.)

related to the CO oxidation activity [6]. There are many researchers focus on doping the CuMnO$_x$ catalyst with different types of metal dopants to improve its catalytic activity [7]. The addition of gold into the CuMnO$_x$ catalyst, the rate of CO oxidation was increased, and the rate of deactivation of the catalyst was reduced [8]. When cerium was doped into transition metal oxides, the in situ forming cerium oxide could promote oxygen storage and release, enhance the oxygen mobility and improve redox property of the catalyst [9].

The copper oxide and supported copper oxides were known to be a highly active for CO oxidation at low temperature [10]. In the major study, we have found that support of CeO$_2$ plays a crucial role in Cu-CeO$_2$ catalyst for the complete oxidation of CO. It is exhibiting a particular activity various orders of magnitude superior to that of conventional Cu-based catalysts comparing with the precious metals [11-12]. In the preparation process, a solution of AuCl$_4$ was added to get the desired pH and gold precipitated into an indistinct support material by controlled addition of a base [13]. The inclusion of gold into nanorods of rutile, specially prepared in a flowerlike structure, has been reported for very high thermal stability (of the gold), most probably due to substantially reduced gold-gold nanoparticle interactions [14].

The addition of low-level promoters into CuMnO$_x$ catalysts has proven beneficial in other oxidation catalysts. The catalyst performance has improved at the higher doping level and it was observed to correlate with the increase in surface area. The ageing precipitate before calcination has marked as the effect on the catalytic activity [15]. The manganese oxide catalysts were high oxygen storage capacities and exhibited high levels of activity in catalytic reactions that result in the elimination of CO by catalytic oxidation [16]. The catalytic activity of CuMnO$_x$ catalyst can be improved for CO oxidation at ambient temperature prepared by inverse co-precipitation method and doping by a small amount of different metal can enhance its activity [17]. The presence of active species of Cu$^+$ makes a strong interaction with ceria to make more oxygen vacancies on the surface of catalyst [18].

In this study, we prepared a series of hopcalite (CuMnO$_x$) catalysts by adding different dopant can enhance the activity of the catalyst for the oxidation of CO [8]. A stagnant air calcination (SAC) of CuMnO$_x$ catalyst doped with (Ce, Ag, or Au) for the synthesis of highly active catalysts was studied for the first time. A tremendous amount of work has been carried out to develop CuMnO$_x$ based catalysts for various applications. The preparation of catalyst has a decisive role in the performance of resulting catalyst. The addition of Au or Ag into the CuMnCeO$_x$ catalyst has resulted in a marked improvement in the catalytic performance. The CuMnCeO$_x$ catalyst doped with Au was more active than the not contain Au. The results and discussions clearly demonstrate the beneficial effect of adding Au to promote CO oxidation activity [23,26]. The objective of this paper is to find out the effect of noble metal doping into CuMnO$_x$ catalyst can modify the CO adsorption ability of the catalyst and affect the catalytic oxidation of CO. The CuMnCeO$_x$ catalyst doped with AuO$_x$ is more active than the CuMnCeO$_x$ catalyst doped with AgO$_x$.

2. Experimental

2.1 Catalyst preparation

The CuMnO$_x$ catalyst was prepared by co-precipitation method. All the chemicals used for the research works were of A.R. grade. A solutions of Mn-Acetate (Mn(CH$_3$COO)$_2$.4H$_2$O) (14.70 g in 33 mL H$_2$O) was added to 3.68 g of copper(II) nitrate (Cu(NO$_3$)$_2$.2.5H$_2$O) and stirred for 1 h. The mixed solution was taken in the burette and added dropwisely to a solution of KMnO$_4$ (6.32 g in 33 mL H$_2$O) under vigorous stirring conditions for co-precipitation purpose [27]. The resultant precipitate was stirred continuously for 2 h. The molar ratio of Cu/Mn in the CuMnO$_x$ catalyst was 1:8.3. The 0.2762 g of ceria was added in the form of cerium nitrate (Ce(NO$_3$)$_2$.6H$_2$O) over the CuMnO$_x$ catalyst at the time of precipitation process so that the ceria concentration was 1.5 % by weight in the final catalyst.

After completing the filtration process, the precipitant was washed several times by hot distilled water to remove all the anions, then after drying the precursors at 110 ^{o}C temperature for 16 h in an oven. The total weight of the precursors was 7.4094 g. After completing, the drying process divided the precursors into two equal's parts according to the weight of the catalyst. In the first part, we added 0.02742 g of AgNO$_3$ as (1 %) in 3.7047 g of CuMnO$_x$ catalyst by wet impregnation method, and the second part; we added 6.49 mL of (0.05 M HAuCl$_4$.3H$_2$O) in 3.7047 g of CuMnO$_x$ by wet impregnation method. The entire precursor was carried out in a furnace at stagnant air calcination conditions at 300 ^{o}C for 2 h to produce the catalyst, and after calcinations, the

catalyst was stored in an airtight glass bottle. The nomenclature of the catalysts thus obtained after calcination process was given below in Table 1.

2.2 Catalyst Characterization

2.2.1 X-ray Diffraction (XRD)

The X-ray diffraction pattern of the catalyst was obtained by using Cu Kα radiation (40 kV, 100 mA) with a Rigaku D/MAX-2400 diffractometer in the range of 2θ of 10° to 80°. The mean crystallite size (*d*) of the phase of catalyst was calculated from line enlargement of the most intense reflection using the Scherrer Equation (1):

$$d = \frac{0.89\,\lambda}{\beta\,cos\theta} \qquad (1)$$

where *d* was the mean diameter of crystallite, and the Scherrer constant was 0.89. The X-ray wavelength ($\lambda = 1.54056$ Å) and the effective line width of the observed X-ray reflection was *β*, calculated by the expression, $\beta^2 = B^2 - b^2$ (where *B* was the full width at half maximum (FWHM), the instrumental broadening was *b*), determined through the FWHM of the X-ray reflection at 2θ of crystalline SiO_2.

2.2.2 Fourier Transforms Infrared Spectroscopy (FTIR)

The Fourier transforms infrared spectroscopy (FTIR) analysis provided a quantitative and qualitative information for organic and inorganic samples. It identifies the chemical bonds presents in a molecule by producing an infrared absorption spectrum. The FTIR analysis was done by Shimadzu 8400 FTIR spectrometer within the range of 400-4000 cm^{-1}.

2.2.3 Scanning electron microscope (SEM-EDX)

Scanning electron microscope (SEM) was a high-resolution electron microscope that produces the image of the sample by scanning it with the help of electron beam. The SEM-EDX was recorded on Zeiss EVO 18 Scanning electron microscope. The EDX was energy dispersive X-ray analyzer it provides information about elemental identification and quantitative composition analysis of different elemental groups present in the catalyst.

2.2.4 N_2 Adsorption-Desorption Isotherm (BET)

The N_2 sorption isotherm was used for determining the specific surface area, pore volume, and pore size distribution of the catalyst. The area of hysteresis loop provides information about the nature of the pores present in the catalyst surfaces. The Micromeritics ASAP 2020 analyzer was used to record the adsorption-desorption isotherm.

2.3 Performance of the catalyst for CO oxidation

The catalytic oxidation of CO was performed under the following reaction conditions: 100 mg of catalyst in the presence of 2.5 vol.% of CO in air maintained at a flow rate of 60 mL/min, with a fixed bed tabular flow reactor. The air was made free from moisture and CO_2 by passing through CaO and KOH pellets drying towers. The reaction temperature was ranged from ambient to 200 °C at a heating rate of 1 °C/min. The microprocessor based temperature controller controlled the rate of heating. The flow rates of CO and air were monitored with the help of digital gas flow meters. Equation 2 can represent the air oxidation of CO over the catalyst.

$$2CO + O_2 \rightarrow 2CO_2 \qquad (2)$$

The gaseous products were analyzed by an online gas chromatograph (Nucon Series 5765) equipped with a methaniser, Porapack Q-column and FID detector for the concentration of CO and CO_2. The catalytic activity was measured for the conversion of CO into CO_2. The conversion of CO at any instant was calculated from values of the concentration of CO in the feed and product steam by the Equation 3, where C_{CO} was the concentration of CO which was proportional to the corresponding area of chromatogram A_{CO}.

$$(X_{CO}) = [(C_{CO})_{in} - (C_{CO})_{out}]/[(C_{CO})_{in}] = \frac{[(A_{CO})_{in} - (A_{CO})_{out}]}{[(A_{CO})_{in}]} \qquad (3)$$

Table 1. The nomenclature of the catalyst samples in this study

Catalyst Name	Nomenclature
$CuMnO_x$	$CuMnO_x$
Ce-doped $CuMnO_x$	CuMnCe
Ag-doped CuMnCe	CuMnCeAg
$AuCl_4$-doped CuMnCe	CuMnCeAu

3. Results and Discussion

3.1 Catalyst characterization

The characterization of the doped and undoped $CuMnO_x$ catalyst reveals the morphology, surface structure, phase identification, material identification and surface area.

3.1.1 Morphology of catalysts

The textural property of the catalysts showed the particle size and morphology of the catalyst. As seen in the SEM micrograph the presence of the particles in a catalyst was comprised of more coarse, coarse, fine, and finest size grains resulted by stagnant air calcination of $CuMnO_x$, CuMnCe, CuMnCeAg, and CuMnCeAu catalyst, respectively. Figure 1(A), (B), (C), and (D) shows the SEM image of $CuMnO_x$, CuMnCe, CuMnCeAg, and CuMnCeAu catalyst, respectively. The entire sample is composed of different size of particles [27]. The SEM image of the catalysts derived from calcinations of these precursors also showed significant decreases [7]. With the help of SEM image, we have obtained the morphology and size of the $CuMnO_x$ particles.

This intermediate mixing of metal oxides can be seen by SEM image (Figure 1), which shows highly mixed CuO, MnO_2, CeO_x, AuO_x, and AgO_x phases. In the presence of higher oxidation state phases could be the result of a greater degree of surface interface between the easily oxidisable Mn-phase and the highly reducible Cu-phase [28].

The particles presence in a CuMnCeAg, and CuMnCeAu catalyst have a fine, less agglomerated, and more homogeneous as compared to other catalyst samples. The size of particles presence in a $CuMnO_x$ catalyst was more coarse, agglomerated, and non-uniform in nature. The particles presence in a CuMnCeAu catalyst has a least agglomerated, fine sized, and uniformly distributed. The crystalline $CuMn_2O_4$ phases have less activity than amorphous ones, and the high activity of doped $CuMnO_x$ catalyst for CO oxidation at a low temperature should attribute to the active amorphous $CuMn_2O_4$ phase.

The addition of Au into the CuMnCe catalyst had a beneficial effect on their stability. The stability was related to the presence of AuO_x within the $CuMnO_x$ catalyst, which also promotes their activity. The stable activity was
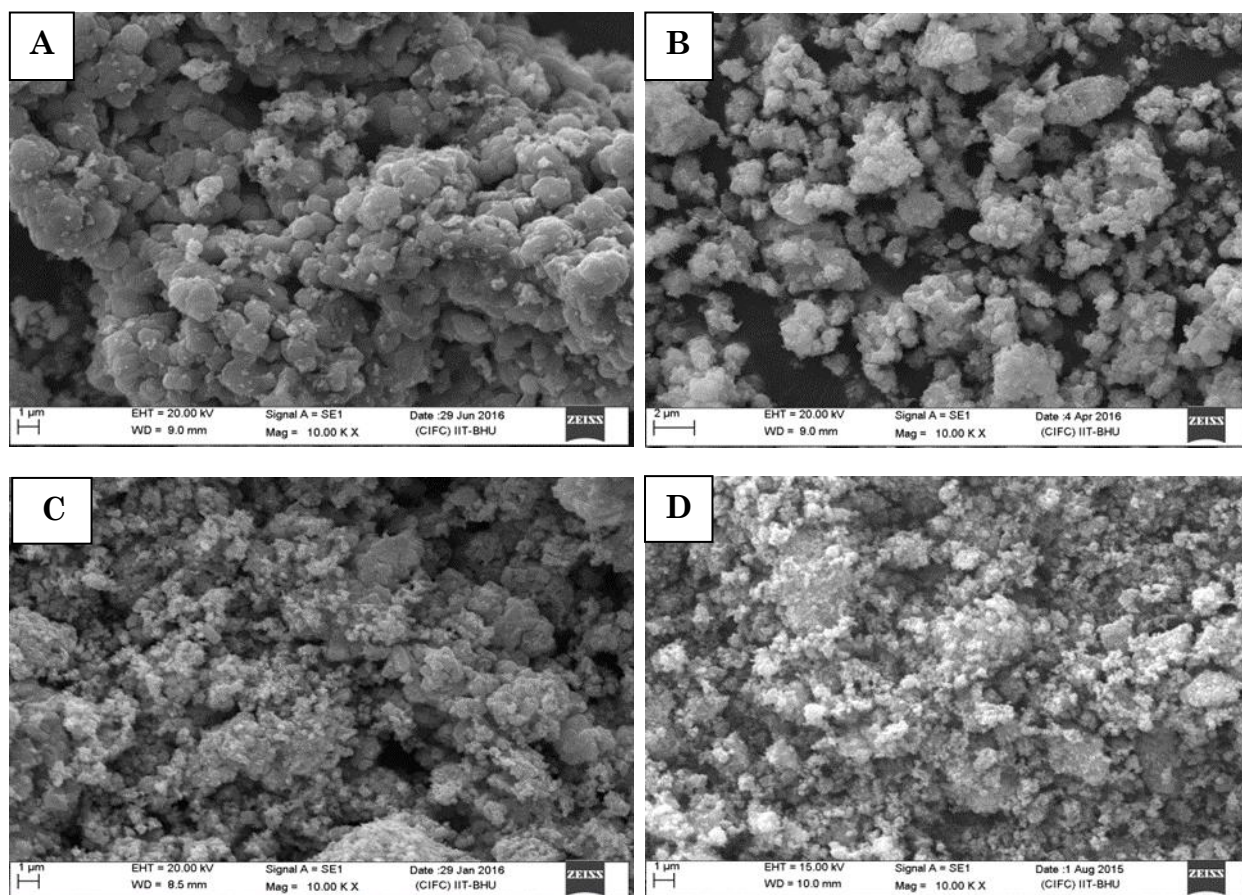
Figure 1. SEM image of the catalysts, A) $CuMnO_x$, B) CuMnCe, C) CuMnCeAg, and D) CuMnCeAu

in clear contrast to other catalysts that have used highly dispersed gold supported on a surface to promote complete oxidation of CO [23]. The activity of the catalyst was increased by the addition of cerium, silver, or gold into the $CuMnO_x$ catalyst. The doping of $CuMnO_x$ catalyst by small amounts of silver or gold was more efficient in improving the catalytic behavior for CO oxidation. For the catalysts with and without gold, there was a consistent decrease of the surface area when the calcination temperature was increased, and this was presumably due to an increase in particle size due to thermal sintering.

3.1.2 Elemental analysis

In the $CuMnO_x$ catalyst, the percentages of different elements were present given by the energy dispersive X-ray (EDX) analysis. The results of EDX showed that all the samples were pure due to the presence of Cu, Mn, O and their relative doping material peaks only as illustrated in Figure 2.

To understand the influence of silver or gold addition on the activity and stability of the promoted $CuMnO_x$ catalysts towards CO oxidation, by EDX characterization technique have been carried out. It was very clear from the EDX analysis that the atomic percentage of Mn was also higher than Cu in the $CuMnO_x$ cata-

lyst. The oxygen content of the CuMnCeAu catalyst was least in comparison to other three prepared catalyst samples. This indicates the presence of oxygen deficiency in the CuMnCeAu catalyst which makes the high density of active sites.

The doping materials associated with $CuMnO_x$ catalyst promote the oxygen storage, release and enhanced the oxygen mobility. It was also apparent that the addition of silver or gold did not significantly alter the textural properties of the catalysts, but the surface area was increased significantly by the additional of gold. This negligible dispersion indicates that the cell unit of ceria was hardly affected by the presence of a dopant element, and therefore it was be concluded that the dispersed among the ceria crystallites not forming a true solid solution. The catalysts obtained by increasing the heating rates during the calcination step present a slightly decreasing catalytic activity. It must be noted that a calcination temperature of the catalysts with the presence of gold higher activities and specific activities than the subsequent gold free $CuMnO_x$ catalyst.

3.1.3 Phase identification and cell dimensions

The XRD analysis of $CuMnO_x$ catalyst doping with Ce, Ag, or Au was individually providing information about the crystalline size and
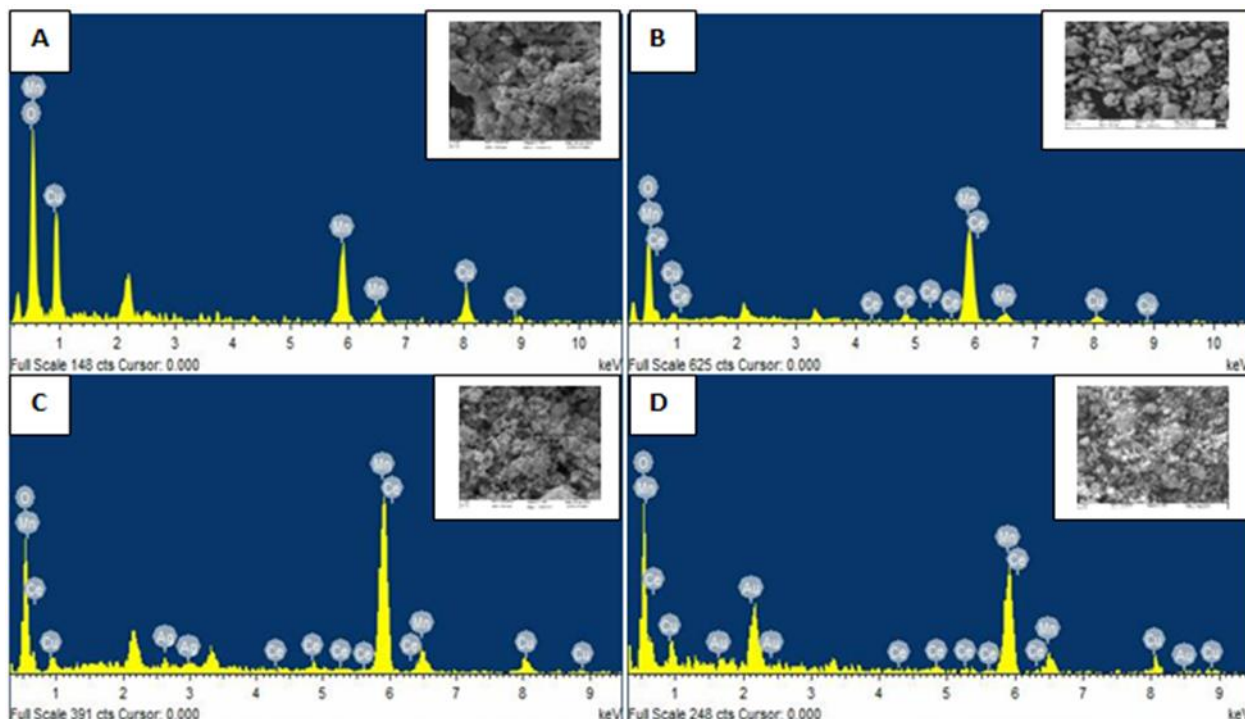
Figure 2. SEM-EDX image of the catalysts, A) $CuMnO_x$, B) CuMnCe, C) CuMnCeAg, and D) CuMnCeAu

coordinate dimensions presence in the catalysts. Figure 3(A), (B), (C), and (D) shows the XRD image of $CuMnO_x$, CuMnCe, CuMnCeAg, and CuMnCeAu catalysts, respectively. XRD analysis of the physically mixed doped and undoped $CuMnO_x$ catalyst was used to determine the final phases after heat treatment at calcination conditions. The $CuMnO_x$ is thought to come from the interaction between the stable re-oxidized CuO phase and MnO_2 phase and their formation taking place due to the metal ion migration at the Cu/Mn oxide phase boundaries to form the spinel structure [28]. The X-ray diffraction patterns of the Au-promoted $CuMnCeO_x$ catalyst is shown in Figure 3(D). The calcined catalyst is between amorphous and crystalline phases could be clearly identified [5].

Spassova and co-workers have reported that an interaction between CuO and MnO_x, with the formation of a highly disordered mixed oxide, is caused by higher catalytic activity [15]. The most intense diffraction peak for metallic Au would be expected at a 2 h value of ca. 36.42, and Au is expected to be present in all the samples mainly as Au^0 since the calcination temperature of 300 ^{o}C leads to the reduction of gold [23].

In the XRD analysis, we have observed that the $CuMnO_x$ catalyst was prepared in stagnant air calcination conditions, their diffraction peak at 2θ was 43.95 and corresponds to its lattice plane (h k l) values was (1 1 1) with JCPDS reference no. (32-0429). The structure was a cubic face-centered $CuMn_2O_4$ phase and crystallite size of the catalyst was 4.70 nm. In the $CuMnO_x$ catalyst doped with (1.5 %) CeO_x in stagnant air calcination conditions their diffraction peak at 2θ was 40.60, and corresponds to its lattice plane (h k l) value was (2 2 1) with JCPDS reference no. (38-0849). The structure was tetragonal-body centered CuO(Mn)Ce phase, and crystallite size of the catalyst was 2.30 nm [25]. In the $CuMnO_x$ catalyst doped with (1.5 % CeO_x) and (1 % AgO_x) prepared in stagnant air calcination conditions and their
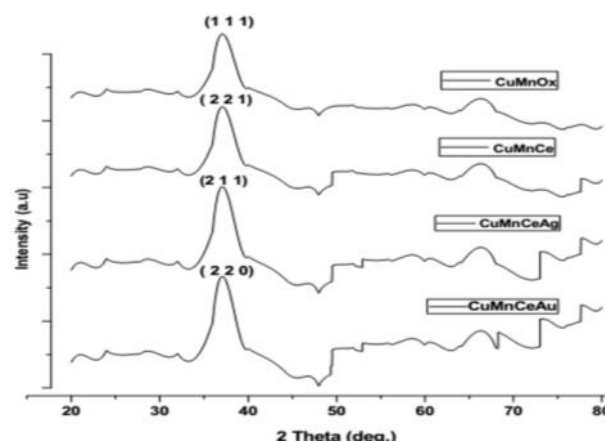

Figure 3. XRD pattern for A) CuMnOx, B) CuMn_Ce, C) CuMn_CeAg, and D) CuMn_CeAu

Table 2. The atomic percentage of a catalyst by EDX analysis

CuMnOx	Cu	Mn	O			Cu/Mn
	30.39	54.46	15.15			0.5580
CuMn_Ce	Cu	Mn	Ce	O		Cu/Mn
	29.81	55.35	1.24	13.60		0.5385
CuMn_CeAg	Cu	Mn	Ce	Ag	O	Cu/Mn
	29.14	57.30	1.14	0.72	11.70	0.5085
CuMn_CeAu	Cu	Mn	Ce	Au	O	Cu/Mn
	29.22	58.70	1.18	0.65	10.25	0.4977

Table 3. The weight percentage of a catalyst by EDX analysis

$CuMnO_x$	Cu	Mn	O			Cu/Mn
	31.38	55.91	12.71			0.5612
CuMnCe	Cu	Mn	Ce	O		Cu/Mn
	30.60	56.90	1.40	11.10		0.5377
CuMnCeAg	Cu	Mn	Ce	Ag	O	Cu/Mn
	30.35	57.45	1.24	0.90	10.06	0.5282
CuMnCeAu	Cu	Mn	Ce	Au	O	Cu/Mn
	29.70	58.90	1.36	0.75	9.29	0.5042

diffraction peak at 2θ was 43.57 and corresponds to its lattice plane (h k l) values was (2 1 1) with JCPDS reference no. (36-0441).

The structure was tetragonal-body centered CuMn(Ce)AgO phase and crystallite size of the catalyst was 2.06 nm. In the $CuMnO_x$ catalyst doped with (1.5 % CeO_x) and (0.5 % AuO_x) in stagnant air calcination conditions and their diffraction peak at 2θ was 36.42 and corresponds to its lattice plane (h k l) values was (2 2 0) with JCPDS reference no. (32-0112). The structure was cubic face centered CuO(MnAu)Ce phase and crystallite size of the catalyst was 1.65 nm.

3.1.4 Identification of the materials

The identification of the metal-oxygen bonds present in the $CuMnO_x$ catalyst doping with (1.5 % CeO_x), (1 % AgO_x), and (0.5 % AuO_x) made by the Fourier transform infrared spectroscopy (FTIR) analysis. The different peak was shown, various types of chemical groups present in the catalyst samples at the invested region (4000-400 cm^{-1}). Figure 4(A), (B), (C), and (D) show the FTIR graph of $CuMnO_x$, CuMnCe, CuMnCeAg, and CuMnCeAu cata-

lyst, respectively. The FT-IR analysis was performed to identify the functional groups of the entire dried sample prior to calcination. From the Figure 4, we get the result that the crystalline phase of doped and undoped $CuMnO_x$ catalyst is existed [15].

The FTIR analysis of $CuMnO_x$ catalyst was prepared in stagnant air calcination conditions, and there are five peaks we have obtained. The transmission spectra at (1640 cm^{-1}) show MnO_2 group, (1280 cm^{-1}) show CO_3^{2-} group, (2350 cm^{-1}) show C=O presence group, (3490 cm^{-1}) show hydroxyl group, and (532 cm^{-1}) shows CuO group presence. The $CuMnO_x$ catalyst doping with (1.5 %) CeO_x at the transmittance conditions were eight peaks obtained. The IR bands (1640 cm^{-1}) show MnO_2, (3490 cm^{-1} and 3900 cm^{-1}) shows OH group, (2120 cm^{-1} and 656 cm^{-1}) shows CuO group, (1180 cm^{-1} and 1080 cm^{-1}) shows the presence of COO group and (2340 cm^{-1}) shows CeO group.

The $CuMnO_x$ catalyst doping with (1.5 %) CeO_x and (1 %) AgO_x (CuMnCeAg catalyst) at the transmittance conditions were seven peaks obtained. The IR band (1640 cm^{-1}) show MnO_2, (2080 cm^{-1}) show AgO, (3510 cm^{-1} and 3060
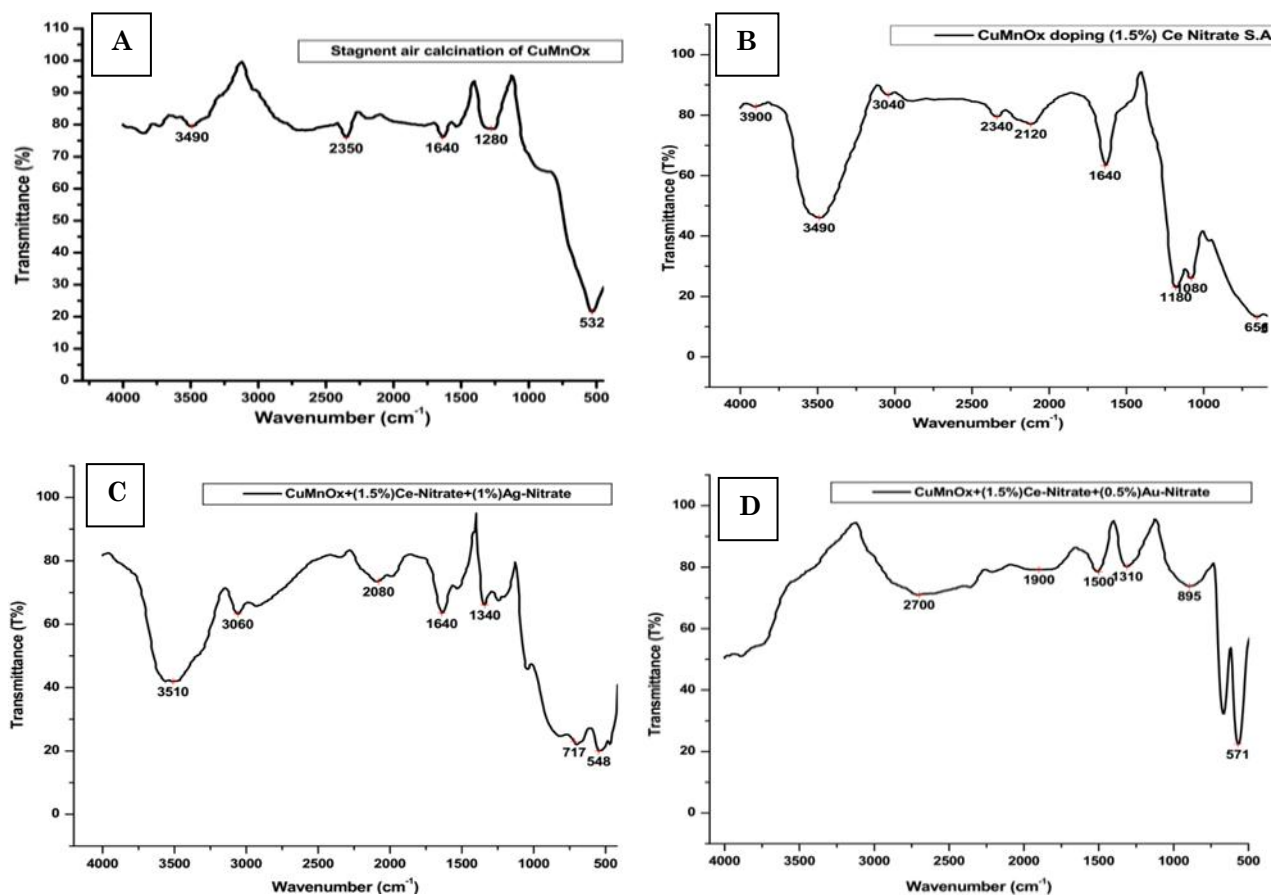
Figure 4. FTIR analysis of A) $CuMnO_x$, B) CuMnCe, C) CuMnCeAg, and D) CuMnCeA$_u$

cm^{-1}) shows OH group, (548 cm^{-1}) shows CuO group, and (717 cm^{-1}) shows CeO group. The CuMnO$_x$ catalyst doping with (1.5 %) CeO$_x$ and (0.5 %) AuO$_x$ (CuMnCeAu catalyst) at the transmittance conditions were five peaks obtained. The IR band of (1900 cm^{-1}) show MnO$_2$, (2700 cm^{-1}) show AuO$_x$, (1310 cm^{-1}) shows OH group, (1500 cm^{-1}) shows Carbonate species, (571 cm^{-1}) shows CuO group, and (895 cm^{-1}) shows CeO group. The spectra of impurities like hydroxyl group (–OH) at 3490 cm^{-1} decreases in the following order: CuMnO$_x$ > CuMnCe > CuMnCeAg > CuMnCeAu. Thus CuMnCeAu was highly pure as compared to CuMnCeAg, CuMnCe, and CuMnO$_x$ catalyst. In all the samples of CuMnO$_x$ catalyst; which originates from the stretching vibrations of the metal-oxygen bond and confirm the presence of CuO and MnO$_2$ phases. The weak band at 1300 cm^{-1} indicates the presence of some carbonaceous group in the catalyst.

3.1.5 Textural properties

The BET surface area of CeO$_x$, AgO$_x$, or AuO$_x$ promoted in CuMnO$_x$ catalyst prepared by SAC route was shown in Figure 5. The total pore volume and specific surface area are two major factors which can affect the catalytic activity for CO oxidation [15]. When the doped and undoped CuMnO$_x$ catalyst catalytic activity was tested, it was found that the CuMnCeAu catalyst has higher surface area and pore volume resulted in the maximum catalytic activity [22,29]. The surface area is a key parameter in determining catalyst activity for CO oxidation. The activity of the catalyst was influenced by the addition of Au into the CuMnO$_x$ oxide catalyst [23].

The surface area of (CuMnCeAu = 192.76 m^2/g) catalyst was much higher than the (CuMnCeAg = 165.45 m^2/g, CuMnCe = 134.70 m^2/g and CuMnO$_x$ = 115.40 m^2/g) catalyst as shown in Table 4. It was also noted that the average pore volume and pore size of CuMnCeAu catalyst was more than the other three prepared catalyst samples in SAC conditions. The average pore diameter increased with increasing calcination temperature because a high-temperature treatment led to particle sintering accompanied with a loss in the active area. The textural properties like surface area, pore volume and pore size of the catalysts were more preferable for the CO oxidation reactions. The larger number of pores presence in a catalyst means a higher number of CO molecules capture on catalyst surfaces, and they show better catalytic activity [12-13].

Clearly, the textural properties of CuMnCeAu catalyst were superior to the other three prepared catalyst samples. In the mesopores, molecules form a liquid-like adsorbed phase having a meniscus of which curvature was associated with the Kelvin equation, providing the pore size distribution calculation. The specific surface area was measured by BET analysis and also following the SEM and XRD studies. Therefore it can be concluded that smaller the particle size larger the surface area. The CuMnCeAg and CuMnCeAu catalyst surface area and pore volume were so high so that it was most active for CO oxidation reaction at a low temperature. The presence of gold in the catalyst increased their stability and reduced deactivation by a trace amount of moisture present in the catalyst.

3.2 Catalyst performance and the activity measurement

The catalyst activity test was carried out to evaluate the effectiveness of different types of doped and undoped CuMnO$_x$ catalyst as a function of temperature. The activity of the catalyst was measured in stagnant air calcination conditions into the laboratory. The CO oxidation by CuMnO$_x$ catalyst was influenced by a combination of factors including preparation method, drying temperature, calcination conditions and the presence of Cu^{2+} and Mn^{2+} near the surface of a catalyst. The interaction between CuO and MnO$_x$ with the formation of a highly disordered mixed metal oxide was the cause of higher catalytic activity for CO oxidation.

Table 4. Textural property of the catalysts by BET analysis

Catalyst	Surface Area (m^2/g)	Pore Volume (cm^3/g)	Ave. Pore Size (Å)
CuMnO$_x$	115.40	0.310	32.55
CuMnCe	134.70	0.365	37.60
CuMnCeAg	165.45	0.410	42.35
CuMnCeAu	192.76	0.428	47.65

The light-off characteristics were used to evaluate the activity of the resulting catalysts with the increasing of the temperature. The characteristic temperature T_{10}, T_{50}, and T_{100} correspond to the initiation of the oxidation, half conversion, and full conversion of CO, respectively. It was evident from the table and figure that the oxidation of CO was just initiated near around the room temperature and higher temperature was necessary for the complete oxidation of CO. In the Figure 6(A), represent the activity of $CuMnO_x$ catalyst in stagnant air calcination conditions and in the Figure 6(B) represent the comparison study of un-doped $CuMnO_x$ and doped $CuMnO_x$ with (1.5 % cerium oxide) catalyst for CO oxidation. It was

evident from the Figure 6(B) that the Ce promoted $CuMnO_x$ catalyst was highly active for the total oxidation of CO at 135 ℃ temperature. A clean surface was exposed by a mixture of CO and air quickly becomes covered with CO since CO requires a single vacant adsorption site. The different effect on the activity of $CuMnO_x$ catalyst due to the addition of CeO_2 by precipitation method was accompanied by an increase in the catalyst surface area.

The CeO_2 phase presence in a $CuMnO_x$ catalyst was accelerating the CO oxidation process due to the availability of the lattice oxygen. The oxidation of CO has initiated over CuMnCe and $CuMnO_x$ catalyst at 25 ℃ temperature. The half conversion of CO over the
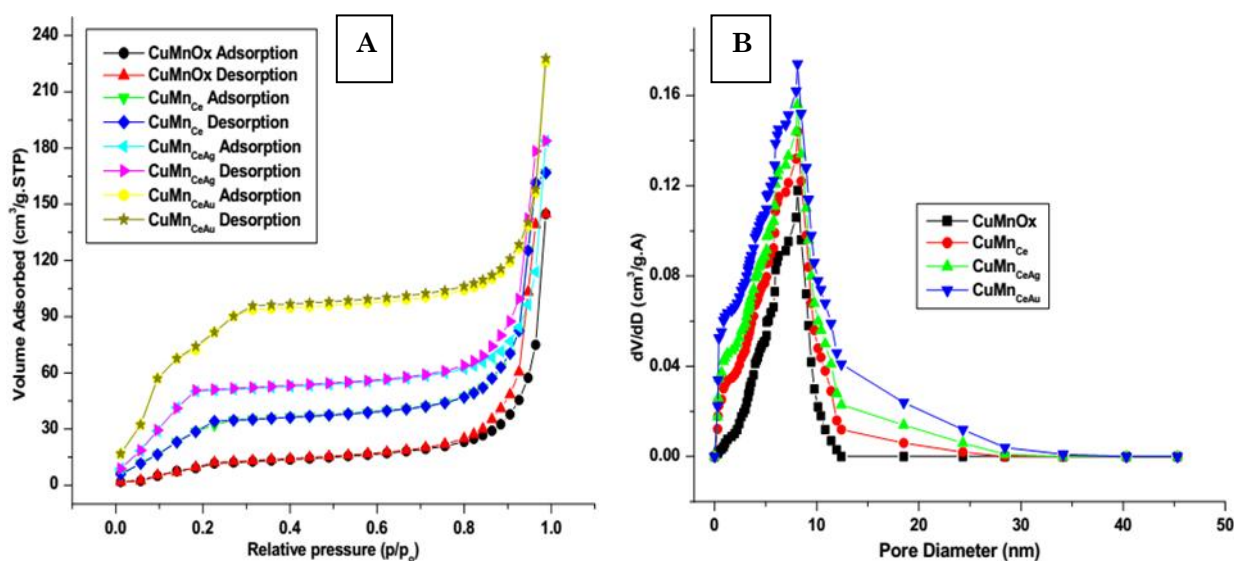

Figure 5. The textural properties A) N_2 adsorption-desorption isotherms, and B) pore size distributions curves
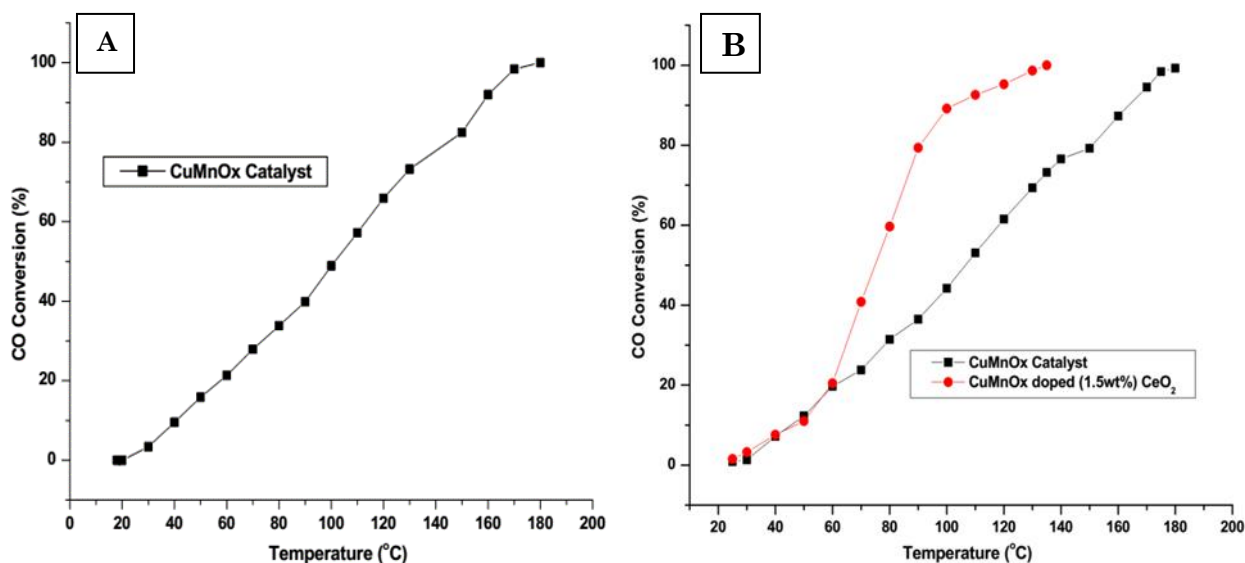

Figure 6. Catalytic activity measurement for (A) $CuMnO_x$ catalyst, (B) $CuMnO_x$, and $CuMnO_x$ doped with Ce-oxide in CuMnCe form

CuMnCe catalyst was 80 °C, which was less than 30 °C over the CuMnO$_x$ catalyst. With the increasing of temperature slightly faster, CO oxidation was observed. The total oxidation temperature of CO was 135 °C for CuMnCe catalyst which was less than 45 °C over the CuMnO$_x$ catalyst.

The addition of AuO$_x$ or AgO$_x$ in the CuMnCe catalyst increases their activity for CO oxidation at low temperature. Thus, the CuMnO$_x$ catalyst promoted with AgO$_x$ or AuO$_x$ and supported with CeO$_2$ shows very high catalytic activity at low temperature. The promoters have shown the greatest effect on the performance of resulting catalyst for CO oxidation. It was expected that the addition of Au introducing the new active sites on the CuMnO$_x$ catalyst. The addition of Au or Ag also increased the reducibility of the catalyst significantly compared to undoped CuMnO$_x$ catalyst. The activity for the surface normalized oxidation rates was similar to the normalized for catalyst mass. Figure 7(A) represents the activity order of CuMnO$_x$ catalyst, CuMnO$_x$ doped with (Ce-oxide) catalyst, and CuMnO$_x$ doped with (1.5 % Ce-oxide and 1 % Ag-oxide) catalyst for CO oxidation. Figure 7(B) represents the activity order of CuMnO$_x$ catalyst, CuMnO$_x$ doped with (1.5 % Ce-oxide) catalyst, and CuMnO$_x$ doped with (1.5 % Ce-oxide and 0.5 % Au-oxide) catalyst for CO oxidation. These Figures 7(B) clearly indicate that Au was not only acting as a structural promoter, which considers the high efficacy of highly dispersed Au particles for low-temperature CO oxidation. The supported noble metal catalysts seem to be quite active for CO oxidation at low temperatures.

The CuMnO$_x$ was a well-known catalyst for the low-temperature CO oxidation process. The accumulation of Ag or Au was highly dispersed in the various oxides form inactive catalyst surfaces at the sub-ambient temperature. The synthesis of highly dispersed Au particles was very sensitive towards the precise preparation methods of the catalyst. The CuMnCe catalyst was highly dispersed in the HAuCl$_4$ solution and highly effective for low-temperature CO oxidation process. The deposition and precipitation were also able to control the distribution, size of the deposited Au particles, and porous structure of the support can be maintained.

The total oxidation temperature of CO was 110 °C for CuMnCeAu catalyst, which was less by 10 °C and 25 °C than that of CuMnCeAg and CuMnCe catalyst, respectively. Therefore, the CuMnCeAu catalyst showed the best catalytic activity in comparison to CuMnCeAg and CuMnCe catalyst in lowering the initial and maximum conversion of CO. The activity order of catalysts match with their characterization results by XRD, FTIR, SEM-EDX, and BET was as follows: CuMnCeAu > CuMnCeAg > CuMnCe > CuMnO$_x$. From the catalytic activity test, we have found out that the promoting Au into the CuMnCe catalyst was a great improvement in their activity. The abundant pores and large surface area present in the AuO$_x$ promoted CuMnCe catalyst has a great potential to further improving their catalytic performance.
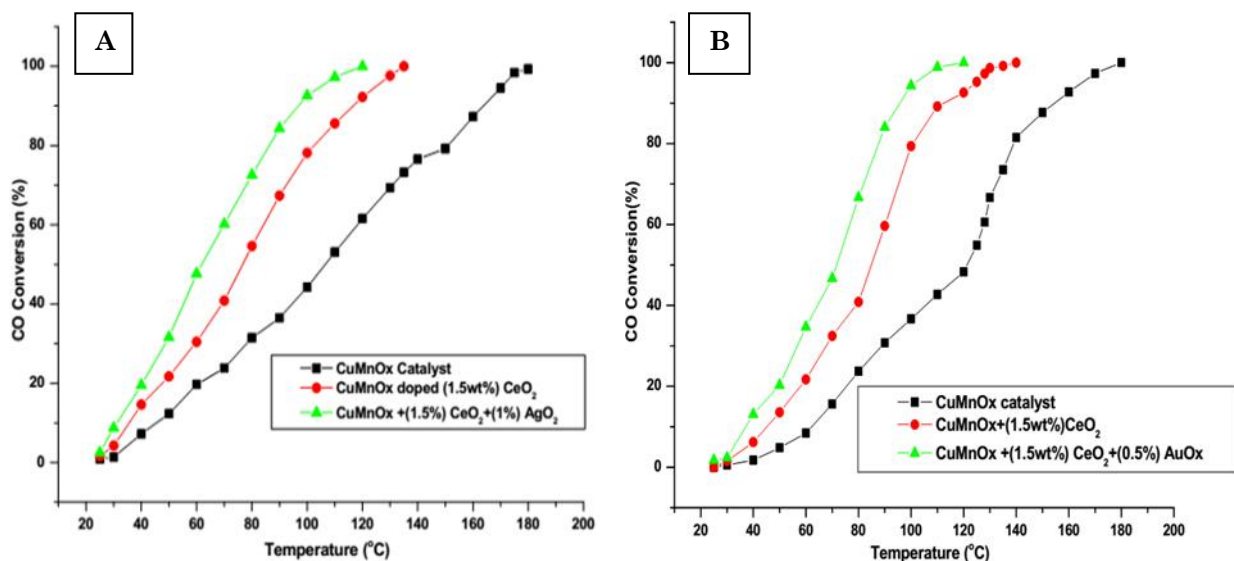

Figure 7. Catalytic activity measurement for (A) CuMnO$_x$, CuMnCe, and CuMnCeAg catalyst, (B) CuMnO$_x$, CuMnCe, and CuMnCeAu catalyst

3.2.1 Final comparison of doped and undoped CuMnO$_x$ catalyst

In comparison between the doped and undoped CuMnO$_x$ catalyst, we have found out that the CuMnO$_x$ catalyst doped with (1.5 %) Ce-Nitrate and (0.5 %) AuCl$_4$ was showed the best result for CO oxidation at low temperature. The presence of CuO$_x$, CeO$_2$, and AuO$_x$ phases in the CuMnCeAu catalyst as evidenced by the XRD and FTIR characterization and may be a possible reason for the higher activity of the catalysts. The introduction of gold will introduce new active sites to the CuMnO$_x$ catalyst that were associated with the gold nanoparticles.

However, the addition of Au into the CuMnCe catalyst also alters the redox property of the catalyst, by increasing their liability to active lattice oxygen species responsible for the CO oxidation [23]. It was proposed that the higher activity of CuMnCeAu catalyst attribute to their amorphous structure, surface area and highly dispersed CeO$_2$ in the lattice which can promote the generation of surface adsorbed oxygen and enhance the mobility of lattice oxygen [26].

Figure 8 represents the comparison study of undoped CuMnO$_x$ catalyst, CuMnO$_x$ catalyst doped with (1.5 % Ce-Oxide), CuMnO$_x$ catalyst doped with (1.5 % Ce-Oxide and 1 % Ag-oxide) and CuMnO$_x$ catalyst doped with (1.5 % Ce-Oxide and 0.5 % AuO$_x$) for CO oxidation. After the comparison study of all doped and undoped of CuMnO$_x$ catalysts, we got the results of the AuO$_x$ or AgO$_x$-doped CuMnO$_x$ catalyst was much active for CO oxidation at low temperature.

In the CuMnCeAu catalyst, a number of oxygen atoms adsorbed during the O$_2$ multipulse was smaller than the amount of CO consumed during the first CO multi-pulse series. The CO multi-pulse experiments have detected two distinct types of active oxygen species participating in the CO oxidation reaction. The first type of active oxygen was observed in a similar amount of both the catalysts and was associated with the mixed oxide catalyst surface. The second type of active oxygen was found only on the Au-doped catalyst; therefore, it was clearly associated with the presence of gold on the catalyst surface.

In Table 5, we have compared the catalytic activity of doped and undoped CuMnO$_x$ catalyst [23]. The full conversion of CO by CuMnO$_x$ catalyst was 180 ^{o}C, but when (1.5 wt.%) CeO$_x$ was doped than the full conversion of CO has occurred at 135 ^{o}C. The addition of AgO$_x$ into the CuMnCe catalyst, the complete conversion of CO was achieved at 125 ^{o}C and the conversion of CO by the addition AuO$_x$ into the CuMnCe catalyst was 110 ^{o}C at stagnant air calcination condition is obtained. The order of activity for the various types of doped and undoped CuMnO$_x$ catalyst for CO oxidation was as follows: CuMnCeAu > CuMnCeAg > CuMnCe > CuMnO$_x$.

The AuO$_x$ was acting like an oxide support, and it was widely accepted that a CO molecule was chemisorbed on an Au atom, while an hydroxyl ion moves from the support to Au(III) ions, creating an anion vacancy. The presence of AgO$_x$ or AuO$_x$ into the CuMnCe catalyst enhances their activity for CO oxidation. The obtained CuMnCeAg catalyst CO conversion was so high but slightly lower than the CuMnCeAu Catalyst. In the catalytic oxidation process, the
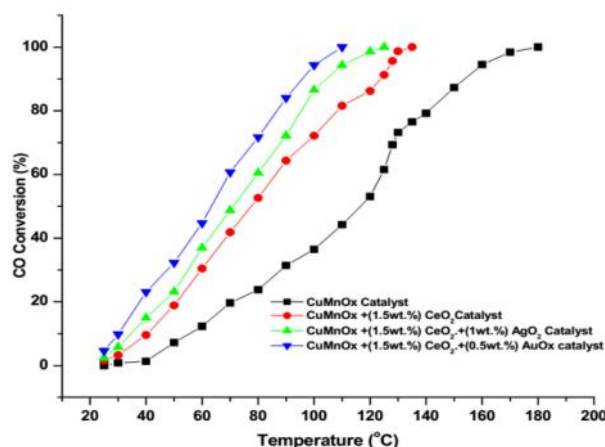

Figure 8. Catalytic activity measurement of the catalysts

Table 5. The comparative study of doped and undoped CuMnO$_x$ catalyst

Catalyst	T$_i$ (^{o}C)	T$_{50}$ (^{o}C)	T$_{100}$ (^{o}C)
CuMnO$_x$	25	102	180
CuMnCe	25	85	135
CuMnCeAg	25	70	125
CuMnCeAu	25	65	110

CO molecules interact with the oxygen species and the resulting vacant oxygen sites were removed by the adsorption of oxygen molecules from the gas phases.

The CO can be regarded as reductive gas, which partially reduces surface sites. The heating of precursor in the oxygen-containing atmosphere (calcination process) may increase the amount of highly active oxygen species presence on the surface of the catalyst. These species was easily removed by the CO molecules and enhance the rate of this process was observed in the temperature range of 50-120 ^{o}C. The catalysts with large surface area show the high initial activity and the elevated temperatures activity of catalysts slightly increases, probably due to a disappearance of such type of organic species. Therefore at the high temperatures, this negative effect decreases due to an enhancement of the redox processes. The addition of AuO_x or AgO_x into the $CuMnO_x$ catalyst their structural property was affected and increases their oxygen mobility [8]. The high activity of $CuMnO_x$ catalyst had been ascribed to the presence of a poorly crystalline phase or amorphous forms of $CuMn_2O_4$. From the Figure 8, it is clearly observed that the performance of the doped catalyst is much better than undoped one. In this paper, we have investigated the incorporation of extra catalyst components to improve their activity for CO oxidation.

When we compare our results to other researchers' results, we have found that the $CuMnO_x$ catalyst with 0.5 wt.% Au added was more active than the Au-free $CuMnO_x$ catalyst [23]. The same result was also observed when the Ag loading 1.0 wt.% on the surface of $CuMnO_x$ catalyst. These experimental data clearly demonstrate the beneficial effect adding of Au or Ag on the surface of $CuMnO_x$ catalyst to promote CO oxidation activity [30]. The CO multi-pulse experiments indicate that two different types of active oxygen species were found to be concerned in the CO oxidation. One type was observed in a similar amount on both doped and undoped $CuMnO_x$ catalysts and was associated with mixed oxide, while the second type was only found on the Au-doped catalyst, and was therefore clearly associated with the presence of gold on the $CuMnO_x$ catalyst surface [26].

4. Conclusions

The oxidation of CO over the various types of doped and undoped $CuMnO_x$ catalyst were significantly influenced by the crystallite size, pore volume, pore size and surface area of the catalyst. The activity of the catalysts was strongly influenced by the presence of AuO_x, AgO_x, and CeO_x oxides on the surface of $CuMnO_x$ catalyst. The doping of smaller amount (1.5 wt%) Ce-oxide into the $CuMnO_x$ catalyst improved their activity for CO oxidation less than 45 ^{o}C compared to undoped $CuMnO_x$ catalyst. Further addition of (1 % AgO_2) into the ($CuMnO_x$ doped (1.5 wt.%) CeO_2) catalyst the activity of catalyst further increased and complete oxidation of CO was observed less than 55 ^{o}C as compared to undoped $CuMnO_x$ catalyst. When (0.5 wt.%) AuO_x addition into the ($CuMnO_x$ doped (1.5 wt.%) CeO_2) catalyst the further activity of the catalyst also increased and the result is that the total oxidation of CO was observed less than 70 ^{o}C as compared to undoped $CuMnO_x$ catalyst.

The addition of noble metal (Ag or Au) on the surface of $CuMnO_x$ catalyst resulted in a marked improvement in the catalytic performance for CO oxidation. The new surface sites created upon doping result in enhanced the catalytic activities for CO conversion over AuO_x or AgO_x supported on CuMnCe catalyst. The nature of support through its morphology and the specific surface area has a significant influence on the performance of catalyst for low-temperature CO oxidation. The addition of AuO_x significantly increases their reducibility of the CuMnCe surface oxygen. It was remarked of high activity at low temperature that has stimulated significant current interest in these types of catalysts. This study has addressed CO oxidation activity of a $CuMnO_x$ catalyst prepared with Au or Ag by a co-precipitation procedure has been investigated.

References

[1] Feng, Y.F., Wang, L., Zhang, Y.H., Guo, Y., Guo, Y.L., Lu, G.Z. (2013). Deactivation Mechanism of $PdCl_2$-$CuCl_2$/Al_2O_3 Catalysts for CO Oxidation at Low Temperatures. *Chinese Journal of Catalysis*, 34: 923-931.

[2] Frey, K., Lablokov, V., Safran, G., Osan, J., Sajo, I., Szukiewicz, R., Chenakin, S., Kruse, N. (2012), Nanostructured MnOx as Highly Active Catalyst for CO Oxidation. *Journal of Catalysis*, 287: 30-36.

[3] Meiyi, G., Nan, J., Yuhong, Z., Changjin, X., Haiquan, S., Shanghong, Z. (2016). Copper-Cerium Oxides Supported on Carbon Nonmaterial for Preferential Oxidation of Carbon Monoxide. *Journal of Rare Earths*, 34: 55-604.

[4] Biabani, A., Rezaei, M., Fattah, Z. (2012). Optimization of Preparation Conditions of Fe-Co Nanoparticles in Low-Temperature CO Oxidation Reaction by Taguchi Design Method. *Journal of Natural Gas Chemistry*, 21: 615-619.

[5] Hutchings, G.J., Mirzaei, A.A., Joyner, R.W., Siddiqui, M.R.H., Taylor, S.H. (1996). Ambient Temperature CO Oxidation Using Copper Manganese Oxide Catalysts Prepared by Co-precipitation: Effect of Ageing on Catalyst Performance. *Catalysis Letters*, 42: 21-24.

[6] Li, J., Zhu, P., Zuo, S.H., Zhou, R. (2010). Influence of Mn Doping on the Performance of CuO-CeO_2 Catalysts for Selective Oxidation of CO in Hydrogen-Rich Streams. *Applied Catalysis A: General*, 381: 261-266.

[7] Mirzaei, A.A., Shaterian, H.R., Joyner, R.W., Stockenhuber, M., Taylor, S.H., Hutchings, G.J. (2013). Ambient Temperature Carbon Monoxide Oxidation Using Copper Manganese Oxide Catalysts: Effect of Residual Na^+ Acting as Catalyst Poison. *Catalysis Communication*, 4: 17-20.

[8] Cole, K.J., Carley, A.F., Crudace, M.J., Clarke, M., Taylor, S.H., Hutchings, G.J. (2010). Copper Manganese Oxide Catalysts Modified by Gold Deposition: The Influence on Activity for Ambient Temperature Carbon Monoxide Oxidation. *Catalysis Letters*, 138: 143-147.

[9] Zhang, X., Ma, K., Zhang, L., Yong, G., Dai, Y., Liu, S. (2010). Effect of Precipitation Method and Ce Doping on the Catalytic Activity of Copper Manganese Oxide Catalysts for CO Oxidation. *Chinese Journal of Chemical Physics*, 24: 97-102.

[10] Liu, W., Flytzani-Stephanopoulos, M. (1995). Total Oxidation of Carbon Monoxide and Methane over Transition Metal-Fluorite Oxide Composite Catalysts I. Catalyst Composition and Activity. *Journal of Catalysis*, 153: 304-316.

[11] Kundakovic, L.K., Stephanopoulos, M.F. (1998), Reduction Characteristics of Copper Oxide in Cerium and Zirconium Oxide Systems. *Applied Catalysis A: General*, 17: 113-29.

[12] Cao, J.L., Wang, Y., Zhang, T.Y., Wu, S.H., Yuan, Z.Y. (2008). Preparation Characterization and Catalytic Behavior of Nanostructure Mesoporous $CuO/Ce_{0.8}Zr_{0.2}O_2$ Catalyst for Low Temperature CO Oxidation. *Applied Catalysis B: Environmental*, 78: 120-128.

[13] Perrault, S.D., Chan, W.C.W. (2009). Synthesis and Surface Modification of Highly Mono Dispersed, Spherical Gold Nanoparticles of 50–200 nm. *Journal of the American Chemical Society*, 131: 17042-17043.

[14] Khoudiakov, M., Gupta, M.C., Deevi, S. (2005). Au/Fe_2O_3 Nanocatalysts for CO Oxidation: A Comparative Study of Deposition–precipitation and Co-precipitation Techniques. *Applied Catalysis A: General*, 291: 151-161.

[15] Cai, L., Hu, Z.B., Li, W. (2014). The Effect of Doping Transition Metal Oxides on Copper Manganese Oxides for the Catalytic Oxidation of CO. *Chinese Journal of Catalysis*, 35: 159-167.

[16] Jones, C., Cole, K.J., Taylor, S.H., Crudace, M.J., Hutchings, G.J. (2009). Copper Manganese Oxide Catalysts for Ambient Temperature Carbon Monoxide Oxidation: Effect of Calcination on Activity. *Journal of Molecular Catalysis A: Chemical*, 305: 121-128.

[17] Sadeghinia, M., Rezaei, M., Amini, E. (2012). Preparation of α-MnO_2 Nano Wires and Its Application in Low Temperature CO Oxidation. *Korean Journal of Chemical Engineering*, 30: 23-29.

[18] Li, L., Chai, S., Binder, A., Brown, S., Yang, S., Dai, S. (2015). Synthesis of MCF-supported AuCo Nanoparticle Catalysts and the Catalytic Performance for the CO Oxidation Reaction. *RSC Advances - Royal Society of Chemistry*, 5: 100212-100222.

[19] Wang, J., Chernavskii, P.A., Wang, Y., Khodakov, A.Y. (2013). Influence of the Support and Promotion on the Structure and Catalytic Performance of Copper-Cobalt Catalysts for Carbon Monoxide Hydrogenation. *Fuel*, 103: 1111-1122.

[20] Wojciechowska, M., Przystajko, W., Zielinski, M. (2007). CO Oxidation Catalysts Based on Copper and Manganese or Cobalt Oxides Supported on MgF_2 and Al_2O_3. *Catalysis Today*, 119: 338-341.

[21] Kramer, M., Schmidt, T.S., Maier, W.F. (2006). Structural and Catalytic Aspects of Sol–Gel Derived Copper Manganese Oxides as Low-Temperature CO Oxidation Catalyst. *Applied Catalysis A: General*, 302: 257-263.

[22] Roy, M., Basak, S., Naskar, M.K. (2016). Bi-template Assisted Synthesis of Mesoporous Manganese Oxide Nanostructures: Tuning Properties for Efficient CO Oxidation. *Physical Chemistry Chemical Physics - Royal Society of Chemistry*, 18: 5253-5263.

[23] Solsona, B., Hutchings, G.J.G., Taylor, S.H. (2004). Improvement of the Catalytic Performance of $CuMnO_x$ Catalysts for CO Oxidation by the Addition of Au. *New Journal of Chemistry*. 28: 708-711.

[24] Tanaka, Y., Utaka, T., Kikuchi, R., Takeguchi, T., Sasaki, K., Eguchi, K. (2003). Water Gas Shift Reaction for The Reformed Fuels

over Cu/MnO Catalysts Prepared via Spinel-Type Oxide. *Journal of Catalysis*, 215: 271-278.

[25] Trivedi, S., Prasad, R. (2016). Reactive Calcination Route for Synthesis of Active Mn–Co_3O_4 Spinel Catalysts for Abatement of CO–CH_4 Emissions from CNG Vehicles. *Journal of Environmental Chemical Engineering*, 4: 1017-1028.

[26] Morgan, K., Cole, K.J., Goguet, A., Hardacre, C., Graham, J., Hutchings, G.J., Maguire, N., Shekhtman, S.O., Taylor, S.H. (2010), TAP Studies of CO Oxidation over $CuMnO_x$ and $Au/CuMnO_x$ Catalysts. *Journal of Catalysis,* 276: 38-48.

[27] Njagi, E.C., Chen, C., Genuino, H., Galindo, H., Huang, H., Suib, S.L. (2010), Total Oxidation of CO at Ambient Temperature Using Copper Manganese Oxide Catalysts Prepared by A Redox Method. *Applied Catalysis B: Environmental*, 99: 103-110.

[28] Kondrat, S.A., Davies, T.E., Zu, Z., Boldrin, P., Bartley, J.K., Carley, A.F., Taylor, S.H., Rosseinsky, M.J., Hutchings, G.J. (2011), The Effect of Heat Treatment on Phase Formation of Copper Manganese Oxide: Influence on Catalytic Activity for Ambient Temperature Carbon Monoxide Oxidation. *Journal of Catalysis*, 281: 279-289.

[29] Bose, P., Ghosh, S., Basak, S., Naskar, M.K. (2016), A Facile Synthesis of Mesoporous NiO Nanosheets and their Application in CO Oxidation. *Journal of Asian Ceramic Society*, 4: 1-5.

[30] Xia, G.G., Yin, Y.G., Willis, W.S. Wang, J.Y. Suib, S.L. (1999), Efficient Stable Catalysts for Low Temperature Carbon Monoxide Oxidation. *Journal of Catalysis*, 185: 91-105.